

ATOMIC HYDROGEN IN A GALACTIC CENTER OUTFLOW

N. M. McCLURE-GRIFFITHS¹, J. A. GREEN¹, A. S. HILL¹, F. J. LOCKMAN², J. M. DICKEY³, B. M. GAENSLER⁴, AND A. J. GREEN⁴

¹ Australia Telescope National Facility, CSIRO Astronomy and Space Science, Marsfield, NSW 2122, Australia; naomi.mcclure-griffiths@csiro.au

² National Radio Astronomy Observatory, Green Bank, WV 24944, USA

³ School of Physics and Mathematics, University of Tasmania, TAS 7001, Australia

⁴ Sydney Institute for Astronomy, School of Physics, The University of Sydney, NSW 2006, Australia

Received 2013 March 27; accepted 2013 April 25; published 2013 May 22

ABSTRACT

We describe a population of small, high-velocity, atomic hydrogen clouds, loops, and filaments found above and below the disk near the Galactic center. The objects have a mean radius of 15 pc, velocity widths of $\sim 14 \text{ km s}^{-1}$, and are observed at $|z|$ heights up to 700 pc. The velocity distribution of the clouds shows no signature of Galactic rotation. We propose a scenario where the clouds are associated with an outflow from a central star-forming region at the Galactic center. We discuss the clouds as entrained material traveling at $\sim 200 \text{ km s}^{-1}$ in a Galactic wind.

Key words: Galaxy: center – ISM: clouds

Online-only material: machine-readable table

1. INTRODUCTION

Many galaxies with active star formation in their central regions have large-scale Galactic winds. These are thought to be responsible for circulating enriched gas to the halo of their host galaxy and even to the intergalactic medium. The galaxy M82 has not only hot, ionized gas in its outflow, but also cool H α emitting filaments (Bland & Tully 1988; Shopbell & Bland-Hawthorn 1998), and cold molecular gas (e.g., Nakai et al. 1987; Taylor et al. 2001). Simulations of starburst winds have shown that dense molecular gas may be entrained in outflowing winds producing cold clouds and filaments at high latitudes around the center of a galaxy (e.g., Cooper et al. 2008; Melioli et al. 2013).

There is increasing evidence that the Milky Way may also have a large-scale nuclear wind. Bland-Hawthorn & Cohen (2003) linked the Galactic center lobe and North Polar Spur to a bipolar wind traced by infrared emission in the inner $\sim 2^\circ$ of the Galaxy. In gamma-ray emission, there are two very large lobes extending to $|b| \sim 60^\circ$, centered on the Galactic center (Su et al. 2010). Recently, Carretti et al. (2013) identified counterparts to the *Fermi* bubbles in radio polarized emission and suggested that the lobes are formed through the effects of massive star formation, which drives a Galactic wind at $\sim 1100 \text{ km s}^{-1}$. There are few direct tracers of the velocity of the putative nuclear wind of the Milky Way, and little evidence of associated cold gas. In fact, the inner 3 kpc of the Milky Way shows a distinct lack of diffuse H I at $|z| < 400 \text{ pc}$, which Lockman (1984) attributed to a Galactic wind removing H I except in the narrow disk (e.g., Bregman 1980). The most convincing kinematic information comes from Keeney et al. (2006) who found high-velocity UV absorption along two sight lines indicating a maximum outflow velocity of 250 km s^{-1} .

We have discovered a population of compact, isolated clouds in the Australia Telescope Compact Array (ATCA) H I Galactic Center Survey that may trace neutral gas in a wind.

2. A POPULATION OF CLOUDS

The ATCA H I Galactic Center Survey (McClure-Griffiths et al. 2012) covers Galactic longitudes $-5^\circ \leq l \leq +5^\circ$, and

Galactic latitude $-5^\circ \leq b \leq +5^\circ$ over the velocity range $-309 \text{ km s}^{-1} \leq V_{\text{LSR}} \leq +349 \text{ km s}^{-1}$ with a velocity resolution of 1 km s^{-1} , an angular resolution of $145''$, and a mean rms H I brightness temperature of $\sigma_{T_b} = 0.7 \text{ K}$.

In the ATCA survey data for the central $1500 \text{ pc} \times 1500 \text{ pc}$ of the Galaxy, there is a population of compact H I clouds that are isolated both spatially and in velocity from the bulk of Galactic H I emission. Clouds were selected to be relatively compact ($\lesssim 0.5$), discrete from other emission, and with brightness temperatures greater than $2\sigma_{T_b}$ over more than five spectral channels. Typically the clouds are only just spatially resolved. However, there are some more extended filamentary features, which we also generally refer to as clouds. Example clouds are shown in Figure 1. We have found a total of 86 clouds between $-209 \text{ km s}^{-1} \leq V_{\text{LSR}} \leq 200 \text{ km s}^{-1}$.

For each cloud we measure the central velocity, V_{LSR} , fitted peak brightness temperature after baseline removal, T_b , velocity FWHM, Δv , mean radius, r , assuming a distance of $R_\odot = 8.5 \text{ kpc}$, peak column density, N_{Hmax} , and cloud mass, M_c . The cloud properties are given in Table 1. The mean radius, $r = \sqrt{A/\pi}$, is calculated from the area of the cloud, A , where A is the number of pixels in the integrated intensity image with $N_{\text{H}} > 0.4 N_{\text{Hmax}}$. This is clearly a very rough estimate, as many clouds are not well represented by an ellipse. The H I masses are calculated as the sum of all pixels greater than 40% N_{Hmax} assuming a distance of 8.5 kpc. We quote H I masses assuming that the gas is optically thin. The FWHM of the H I line is shown in Figure 2, along with histograms of mass, radius, and column density for these clouds. The median, minimum, and maximum values for the population are given in Table 2. There are no strong correlations of cloud radius, FWHM, or mass with z height. The median line width corresponds to $T_k \equiv 22\Delta v^2 \leq 4000 \text{ K}$. Assuming that the unresolved clouds are roughly spherical, we estimate an average H I number density, $\langle n_c \rangle \sim N_{\text{H}}/(2r) = 1 \text{ cm}^{-3}$.

There are several larger features, such as the loop at $(l, b) = (359^\circ, -3^\circ)$ (Figure 1(d)), which appear to be cohesive over many degrees. These features also have larger velocity widths and velocity gradients. The $(l, b) = (359^\circ, -3^\circ)$ loop is particularly interesting because it appears to point directly back to the Galactic center.

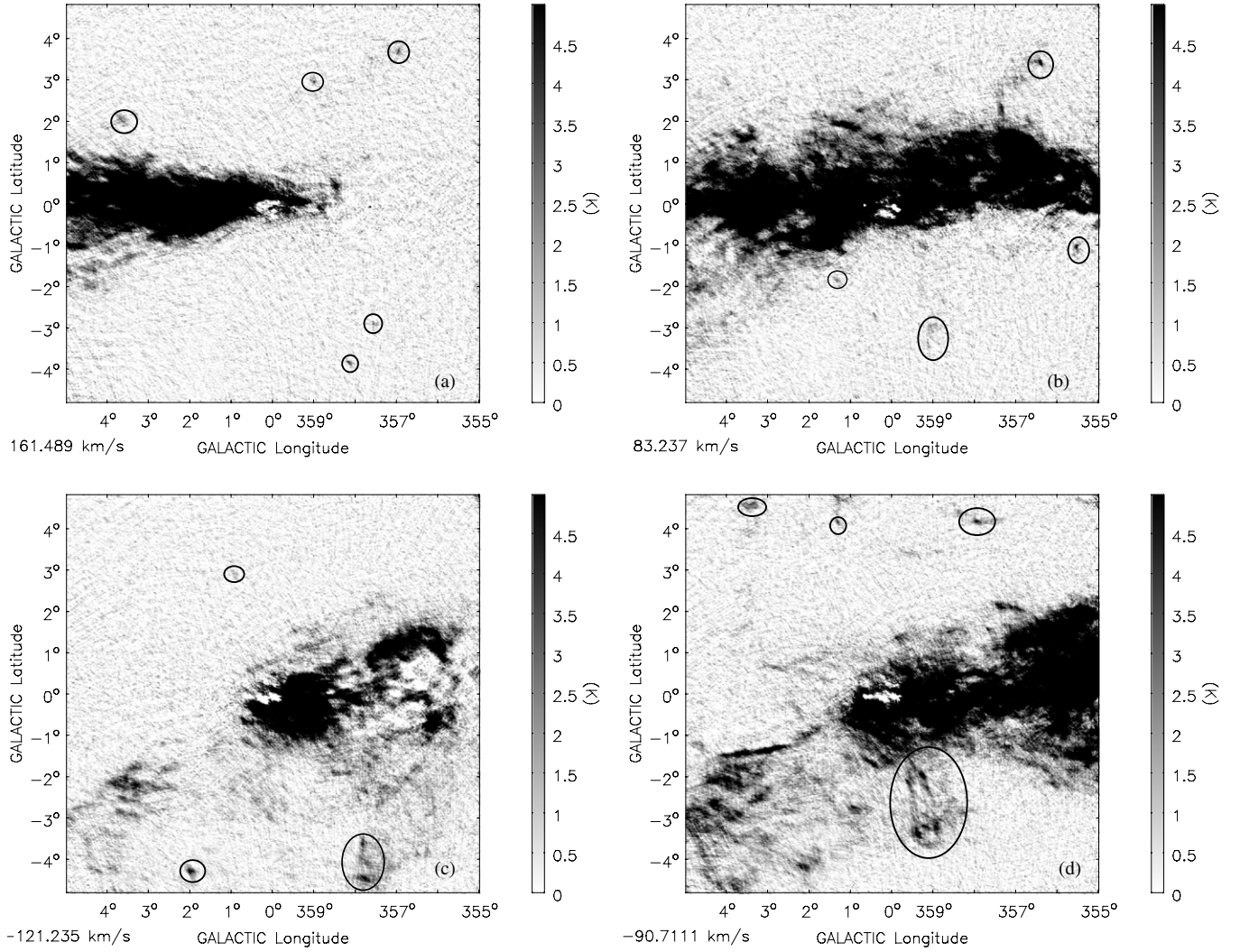


Figure 1. H I images at (a) $v = 161.5 \text{ km s}^{-1}$, (b) $v = 83.2 \text{ km s}^{-1}$, (c) $v = -121.2 \text{ km s}^{-1}$, and (d) $v = -90.7 \text{ km s}^{-1}$. The cataloged clouds whose central velocity lies within 5 km s^{-1} of the shown velocity are circled.

Table 1
Compact Clouds Catalog

Name	l (deg)	b (deg)	V_{LSR} (km s^{-1})	Peak T_b (K)	Δv (km s^{-1})	N_{Hmax} ($\times 10^{19} \text{ cm}^{-2}$)	M_c (M_{\odot})	r (pc)
G0.2+3.8+65	0.23	3.81	63.7	4.4	5.9	5.7	25	6.6
G0.2-1.6-170	0.27	-1.62	-169.6	4.9	17.5	17.6	2190	32.9
G0.3+2.8+195	0.30	2.84	200.8	1.4	28.6	9.7	220	12.2
G0.3+3.7-82	0.36	3.74	-74.3	3.7	13.7	11.1	706	22.4
G0.7+4.5+61	0.68	4.52	63.3	9.6	5.3	10.8	287	14.2

(This table is available in its entirety in a machine-readable form in the online journal. A portion is shown here for guidance regarding its form and content.)

2.1. Cloud Kinematics

The location of the clouds, color-coded by their local standard of rest (LSR) velocities, is shown in Figure 3(a). The clouds clearly do not follow Galactic rotation. The velocity projection of an object at l, b onto the LSR can be written as

$$V_{\text{LSR}} = \left[R_0 \sin l \left(\frac{V_{\theta}}{R} - \frac{V_{\odot}}{R_{\odot}} \right) - V_R \cos(l + \theta) \right] \times \cos b + V_z \sin b, \quad (1)$$

where θ is defined around the Galactic center in a clockwise direction from the Sun–Galactic center line. The velocity terms V_R , V_{θ} , and V_z are the radial, azimuthal, and vertical velocities. In circular Galactic rotation, V_R and V_z are zero and the $\sin l$ term produces a change in sign of V_{LSR} across $l = 0^{\circ}$. The absence of this signature in the cloud distribution suggests that the kinematics of the clouds are not dominated by circular Galactic rotation. Because the clouds are at high velocities and do not show the signature of Galactic rotation, we assume that the clouds are located at the Galactic center.

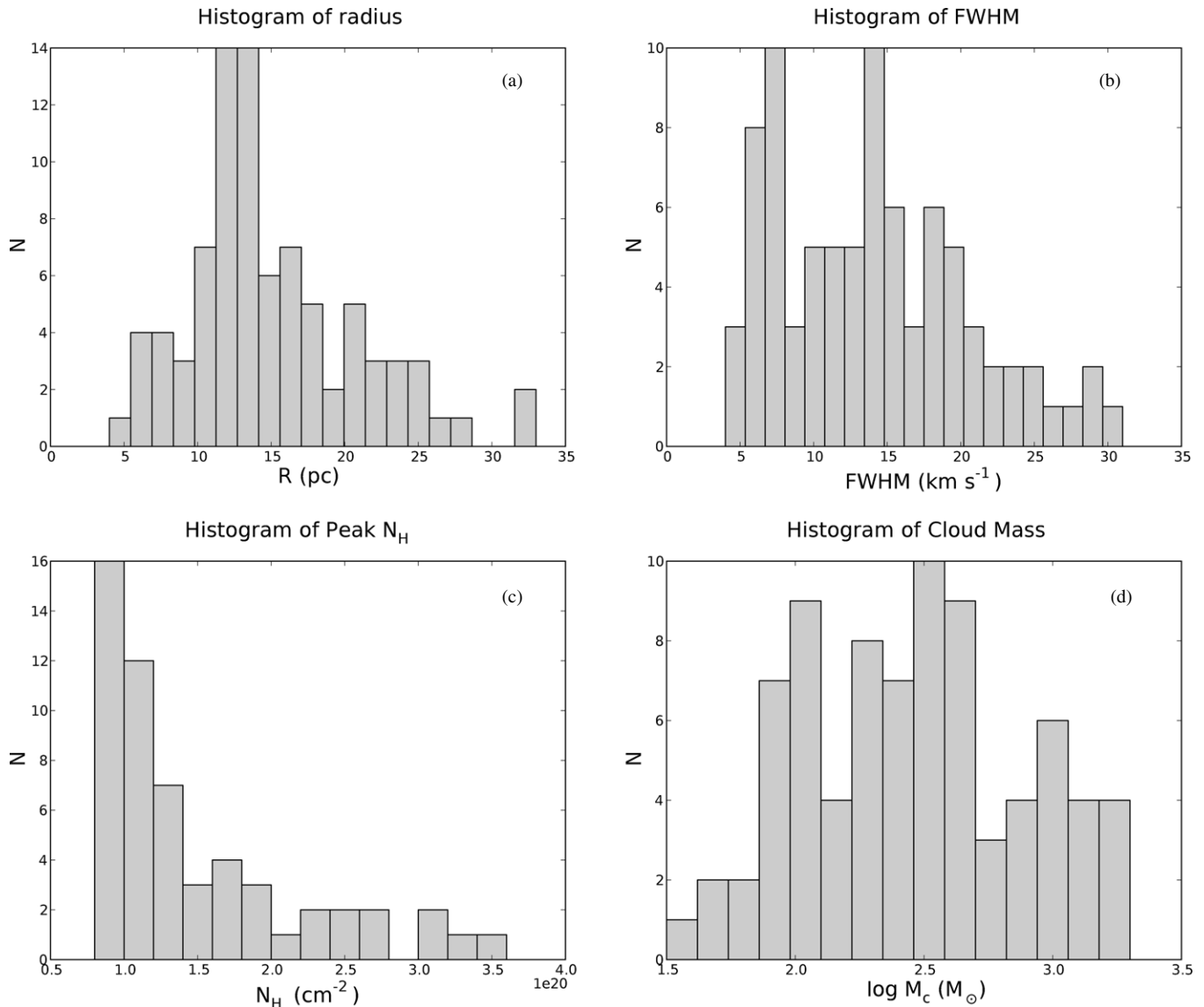


Figure 2. Histograms of (a) the mean radius of individual clouds, (b) the velocity FWHM of the clouds, (c) the peak column density, N_{H} , of the clouds, and (d) the total mass of the clouds.

Table 2
Cloud Population Properties

Property	Median	Min	Max
r (pc)	15.0	3.5	32.9
Δv (km s^{-1})	13.6	3.0	30.9
T_b (K)	3.8	1.4	14.2
N_{Hmax} (10^{19} cm^{-2})	9.9	1.0	34.9
M_c (M_{\odot})	270	5	2.1×10^3

Clouds above the Galactic plane have predominantly positive velocities, while clouds below the Galactic plane have predominantly negative velocities. Above the plane, there are 16 clouds at negative velocities and 29 clouds at positive velocities. Below the plane, there are 28 clouds at negative velocities and 13 clouds at positive velocities. The mean LSR velocity at positive latitudes is 40.7 km s^{-1} and the mean velocity at negative latitudes is -52.8 km s^{-1} . This is unlikely to be the effect of the V_z term in Equation (1), as $\sin b$ is very small and would require V_z values of $5000\text{--}10,000 \text{ km s}^{-1}$ to explain the observed range of LSR velocities.

This kinematic asymmetry is likely a product of confusion with unrelated H I emission, which affects our ability to find isolated clouds. It is well known that most of the H I emission around the Galactic center at $v_{\text{LSR}} > 100 \text{ km s}^{-1}$ is at $l > 0^\circ$ and $b < 0^\circ$, and similarly the emission at $v_{\text{LSR}} < -100 \text{ km s}^{-1}$ is at $l < 0^\circ$ and $b > 0^\circ$ (Burton & Gordon 1978; see also Figure 4 of McClure-Griffiths et al. 2012). Consequently, we are not likely to find many high-velocity clouds isolated in l - b - v space with positive velocities at $b < 0^\circ$ or with negative velocities at $b > 0^\circ$.

2.2. Simulated Population

To understand the selection effects on the distribution of observed cloud velocities, we have simulated clouds in an outflowing wind. We have populated the interior of two cones having an opening angle, α , centered on the Galactic center and extending to a height of 1.5 kpc with 1000 randomly distributed clouds. Each cloud was assigned an LSR velocity based on its location, a constant conical wind of velocity, V_w , and the

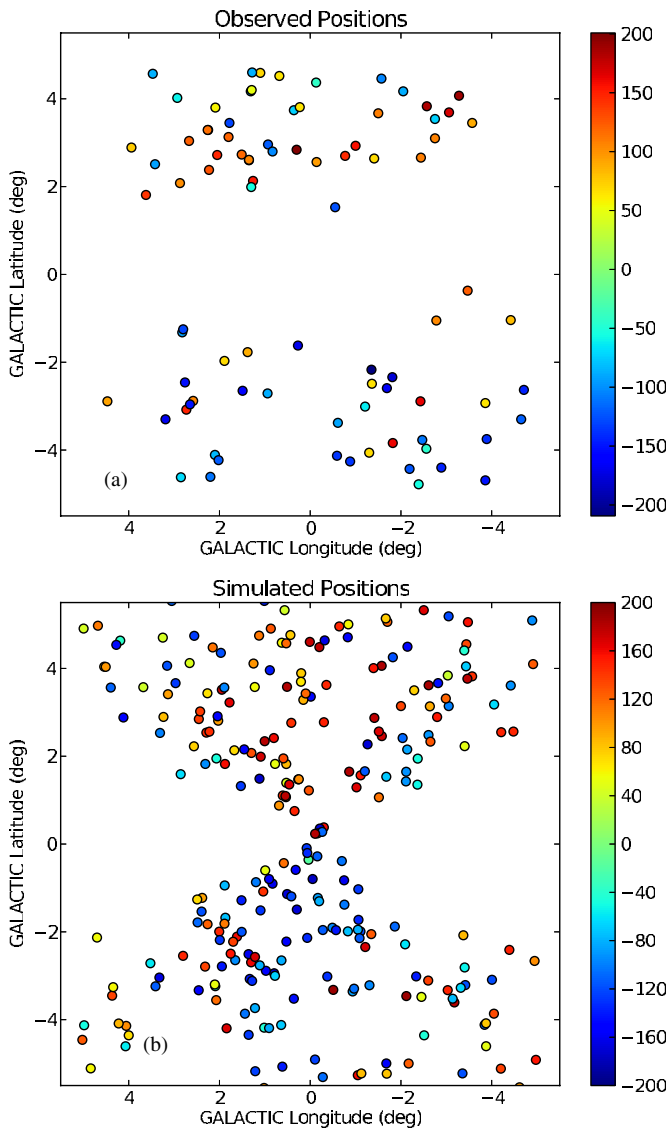


Figure 3. Distribution of clouds around the Galactic center found in (a) the ATCA Galactic center survey and (b) a simulated wind of velocity 190 km s^{-1} . The color of the symbols is determined by the central velocity of the sources. The LSR velocity of the simulated clouds is calculated from Equation (2).

expression similar to that derived by Keeney et al. (2006),⁵

$$V_{\text{LSR}} = V_w \left[\frac{\rho}{r} (1 - \cos^2 b \cos^2 l) \mp \cos b \cos l \right. \\ \left. \times \left[1 - \frac{\rho^2}{r^2} (1 - \cos^2 b \cos^2 l) \right]^{1/2} \right] - 220 \sin l \cos b. \quad (2)$$

Here l and b are the Galactic coordinates, ρ is the distance along the line of sight to a cloud, r is the cloud's distance from the Galactic center, and $r^2 = R_\odot^2 - 2\rho R_\odot \cos b \cos l + \rho^2$. The second term is negative for objects on the near side of the

Galactic center and positive for objects on the far side of the Galactic center from the Sun. We assumed the IAU standard $R_\odot = 8.5 \text{ kpc}$.

Each simulated cloud was compared to the HI actually detected in the ATCA survey at its l and b . If the cloud was located at a velocity where there was no significant HI emission ($< 4\sigma_{T_b}$), it was assumed to have been “detected.” Models covered wind velocities, V_w , between 100 km s^{-1} and 800 km s^{-1} . Wind velocities $\lesssim 150 \text{ km s}^{-1}$ are unable to produce high-velocity clouds as observed, whereas large wind velocities produce a cloud distribution whose mean velocity is higher than observed. Using a Kolmogorov–Smirnov (K-S) test, and separating the data into positive and negative latitude regions, we estimated the probability that the velocities of the observed clouds could be drawn from the same distribution as the simulated clouds. The K-S test p -values as a function of V_w showed a peak near $V_w \sim 190 \text{ km s}^{-1}$ for positive latitudes and near $V_w \sim 220 \text{ km s}^{-1}$ for negative latitudes, but at a lower confidence level. For all V_w , the simulated velocities were more consistent with the observed velocity distribution at positive latitudes than at negative latitudes. Adopting a threshold of $p < 0.05$, the K-S test implies that wind velocities greater than 270 km s^{-1} and less than 150 km s^{-1} are not consistent with the observed cloud velocities.

The observed cloud longitudes and latitudes set a lower limit on the cone opening angle, α . Values $\alpha \lesssim 3\pi/4$ radians are too narrow to produce intermediate latitude ($|b| \approx 2^\circ$) clouds at $|l| > 4^\circ$. The upper limit to α is not well constrained as there is coupling between the angle and the assumed wind velocity. We experimented with several angles, including a fully spherical distribution, and found the results were best matched to $\alpha = 3\pi/4$ radians.

The resulting “detected” clouds for a wind velocity of $V_w = 190 \text{ km s}^{-1}$ and $\alpha = 3\pi/4$ are shown in Figure 3(b). Although the mean velocity of the initial distribution at both positive and negative latitudes was close to zero, because of the selection effects from blending with unrelated HI emission, the velocity distribution of the detected clouds shows the same preference for positive velocities at $b > 0^\circ$ and negative velocities at $b < 0^\circ$ observed in the real clouds. From 50 realizations of the simulation with $V_w = 190 \text{ km s}^{-1}$, we find mean and median positive latitude velocities of 52 km s^{-1} and 88 km s^{-1} , and mean and median negative latitude velocities of -4 km s^{-1} , and -60 km s^{-1} , respectively. The real data have mean and median values, respectively, of 40.7 km s^{-1} and 75.4 km s^{-1} at $b > 0^\circ$, and -52.8 km s^{-1} and -93.3 km s^{-1} at $b < 0^\circ$. The velocity discrepancies at negative latitudes may indicate a higher wind velocity below the Galactic plane or a wind that does not point directly down.

The simulation produces a large number of clouds at small longitudes ($-1^\circ \lesssim l \lesssim +1^\circ$) and small velocities $-70 \text{ km s}^{-1} \lesssim V_{\text{LSR}} \lesssim +70 \text{ km s}^{-1}$ at all latitudes. These clouds are collimated along the wind axis perpendicular to the Galactic plane. In most cases, we expect these to be blended with unrelated low-velocity HI emission. However, examining the observed HI data cube we do find significant structure collimated perpendicular to the Galactic plane at $-1^\circ \lesssim l \lesssim +1^\circ$ with velocities $|V_{\text{LSR}}| \sim 50\text{--}70 \text{ km s}^{-1}$. These features do not meet our criteria of being discrete from other emission and were therefore not cataloged, but may reasonably be part of the same wind structure.

The simulation thus approximately reproduces some of the key features of the observed distribution. The observations are

⁵ This is a near reproduction of Equation (1) from Keeney et al. (2006) except the second term is raised to the power of 1/2, correcting a typographical error in Keeney et al.

consistent with an outflowing conical wind of $\sim 200 \text{ km s}^{-1}$. We are also able to say with confidence that the observed velocity distribution of clouds with positive velocities at $b > 0^\circ$ and negative velocities at $b < 0^\circ$ is caused by confusion with unrelated H I.

3. DISCUSSION AND CONCLUSIONS

The recent discovery of the *Fermi* bubbles (Su et al. 2010) in γ -ray emission and their apparent counterparts in polarized radio continuum (Carretti et al. 2013) has fueled speculation that either there is a powerful jet from the Galactic center or there has been a past burst of star formation. In explaining the polarized radio continuum structure of the *Fermi* bubbles, Carretti et al. (2013) argue that the bubbles are consistent with a past burst of star formation and confirm the Bland-Hawthorn & Cohen (2003) estimate that the bubbles required an injection of $\sim 10^{55}$ erg. They estimate that the interiors of the *Fermi* bubbles are filled with hot plasma of temperature $T_w \sim 10^7$ K with a density, $n_w \sim 9 \times 10^{-3} \text{ cm}^{-3}$, traveling at a velocity of 1100 km s^{-1} .

The median radius, column density, and velocity width of the Galactic center H I are very similar to the lower halo tangent point clouds identified by Ford et al. (2010) and Lockman (2002). Ford et al. (2010) suggested that halo clouds are the remnants of supershells and superbubbles pushed beyond the Galactic disk through the stellar winds and supernovae of massive stars, but remaining dynamically linked to the Galactic disk. Our Galactic center clouds have higher velocities than the Ford et al. (2010) clouds. The formation mechanism for the Galactic center clouds, which determines their dynamics, is therefore probably more energetic than for the halo clouds. This is not surprising; the star formation rate in the inner 100 pc of the Galaxy is $0.1 M_\odot \text{ yr}^{-1}$ (reviewed by Crocker 2012), whereas the star formation rate at the end of the Galactic bar where many halo clouds were found ($l \approx 30^\circ$) is $\sim 10^{-4} M_\odot \text{ yr}^{-1}$ (Veneziani et al. 2013).

In spite of the extreme star formation rate in the very active region of the Galactic center and estimated high temperatures in the wind, cold clouds are not unexpected. Simulations by Cooper et al. (2008) of starburst-driven Galactic winds show compact clouds, filaments, and complex structures of density, $n \sim 10 \text{ cm}^{-3}$, and temperature, $T \sim 10^4$ K, entrained in the inner 400 pc of a starburst wind. Similarly, the Melioli et al. (2013) simulations of the M82 wind produced a wealth of features at $T \sim 10^4$ K with sizes 20–300 pc and densities in the range 10^{-1} – 10 cm^{-3} . The velocity of this cold phase of the outflow is typically 10%–30% of the velocity of the hot phase, or 100–800 km s^{-1} , for the Cooper et al. (2008) and Melioli et al. (2013) models. Melioli et al. (2013) also found that in order for the wind to contain a rich filamentary structure of cool gas, the starburst needed to occur over a relatively short timescale of a few million years.

Our wind velocity modeling produces a velocity of the cold component of the wind that is similar to that observed in the H α emitting filaments of M82 (Shopbell & Bland-Hawthorn 1998) and predicted by hydrodynamic simulations (Cooper et al. 2008; Melioli et al. 2013). We can estimate the velocity of the hot component using the relationship for the ratio of the terminal velocity of the cold clouds, V_t , to the hot wind, V_{hw} , for a cloud of density, n_c , in a wind of density, n_w , (Martin 2005):

$$\frac{V_t}{V_{hw}} \simeq \left[\frac{3n_w}{2n_c} \right]^{1/2}. \quad (3)$$

Assuming $V_t = V_w = 190 \text{ km s}^{-1}$, as derived in Section 2.2, we estimate the velocity of the hot wind as $V_{hw} \sim 1600 \text{ km s}^{-1}$, which is consistent with the hot wind velocity of 1100 km s^{-1} estimated by Carretti et al. (2013).

Presuming that the clouds are launched from very near the galactic plane, to reach 4° latitude in a $\sim 200 \text{ km s}^{-1}$ wind takes at least 3 Myr. If the clouds are entrained in a hot wind, then they will be subject to a number of destructive effects. First, they will evaporate. The evaporation rate, \dot{m} , for an unmagnetized 15 pc cloud in a 10^7 K plasma with a density of $n_w \sim 9 \times 10^{-3} \text{ cm}^{-3}$ is $\dot{m} \sim 1 \times 10^{-3} M_\odot \text{ yr}^{-1}$, assuming saturated evaporation (Cowie et al. 1981). This implies a typical survival time of a few $\times 10^5$ yr, which is less than the time for a cloud to reach a z height of 400 pc in a 200 km s^{-1} wind. However, the evaporation timescale is highly sensitive ($\propto T^{5/2}$) to the assumed temperature of the plasma surrounding the clouds. Hydrodynamic models of winds show that the temperature may be anywhere in the range few $\times 10^{6-7}$ K; it therefore seems possible that the clouds could survive for up to ~ 1 Myr. Also important to the clouds' lifetimes are the cloud crushing time, due to the wind shock, and the cloud cooling time. The relative timescales for these two effects give an estimate of whether the cold, dense clouds would be protected by an enveloping radiative shock (Cooper et al. 2008). The cooling time for a cloud of density n_c of shocked temperature $T_{cl,sh} = 3/16 T_w (n_w/n_c)$ is on the order of a few hundred years. This is much less than the cloud crushing time, $t_{cc} \approx (n_c/n_w)(r_c/v_w) \sim 4 \text{ Myr}$ (Cooper et al. 2008), which suggests that a cloud could survive for some time in the hot wind.

The total mass of H I in the observed clouds is only $\sim 4 \times 10^4 M_\odot$. The mass-loss rate, assuming the oldest cloud is ~ 4 Myr, is $0.01 M_\odot \text{ yr}^{-1}$. At this rate it is unlikely that this outflow will have a significant impact on the $\sim 3 \times 10^7 M_\odot$ reservoir of cold gas estimated for the 100 pc ring in the Central Molecular Zone (Molinari et al. 2011). We estimate the work required to accelerate these clouds to their current velocities; for a $270 M_\odot$ cloud traveling at 200 km s^{-1} , the kinetic energy is $\sim 1 \times 10^{50}$ erg, and the kinetic energy of the most massive cloud in our sample is $\sim 8 \times 10^{50}$ erg. The total estimated kinetic energy for all clouds traveling at a velocity of 200 km s^{-1} is $\sim 1.5 \times 10^{52}$ erg. Assuming the ratio of kinetic energy of the H I clouds to the total input wind energy is ~ 0.2 (Weaver et al. 1977), as often assumed for superbubbles, the required wind energy input was $\sim 8 \times 10^{52}$ erg over the past 10^6 yr. The wind luminosity is therefore $\sim 2 \times 10^{39} \text{ erg s}^{-1}$, which is easily supplied through supernovae and stellar winds in the Galactic center region with a star formation rate of $\sim 0.1 M_\odot \text{ yr}^{-1}$ (Crocker 2012).

4. SUMMARY

We have identified a population of compact, cool, $T < 4000$ K, H I clouds around the Galactic center. Although physically similar in terms of size, temperature, and column density to other cold H I clouds in the lower halo of the Galaxy, the Galactic center H I clouds have unique kinematics and do not follow Galactic rotation. We suggest that these clouds are associated with a wind from the Galactic center and are the remnants of cold, dense gas entrained in the outflowing wind. Using a simple model for a Galactic wind with a velocity of $\sim 200 \text{ km s}^{-1}$, we are able to roughly reproduce the observed velocity distribution of the clouds. From the 200 km s^{-1} velocity of the cold phase gas, we estimate that the hot wind

emanating from the Milky Way's center must have a velocity of $\sim 600\text{--}1900\text{ km s}^{-1}$. We estimate the luminosity required to drive the clouds is $\sim 2 \times 10^{39}\text{ erg s}^{-1}$, which is easily supplied by stellar winds and supernovae in the Galactic center region over the past $\sim 2 \times 10^6\text{ yr}$.

We are grateful to R. Crocker for useful comments on an early draft of this manuscript. The ATCA is part of the Australia Telescope which is funded by the Commonwealth of Australia for operation as a National Facility managed by CSIRO.

REFERENCES

- Bland, J., & Tully, B. 1988, *Natur*, **334**, 43
 Bland-Hawthorn, J., & Cohen, M. 2003, *ApJ*, **582**, 246
 Bregman, J. N. 1980, *ApJ*, **236**, 577
 Burton, W. B., & Gordon, M. A. 1978, *A&A*, **63**, 7
 Carretti, E., Crocker, R. M., Staveley-Smith, L., et al. 2013, *Natur*, **493**, 66
 Cooper, J. L., Bicknell, G. V., Sutherland, R. S., & Bland-Hawthorn, J. 2008, *ApJ*, **674**, 157
 Cowie, L. L., McKee, C. F., & Ostriker, J. P. 1981, *ApJ*, **247**, 908
 Crocker, R. M. 2012, *MNRAS*, **423**, 3512
 Ford, H. A., Lockman, F. J., & McClure-Griffiths, N. M. 2010, *ApJ*, **722**, 367
 Keeney, B. A., Danforth, C. W., Stocke, J. T., et al. 2006, *ApJ*, **646**, 951
 Lockman, F. J. 1984, *ApJ*, **283**, 90
 Lockman, F. J. 2002, *ApJL*, **580**, L47
 Martin, C. L. 2005, *ApJ*, **621**, 227
 McClure-Griffiths, N. M., Dickey, J. M., Gaensler, B. M., et al. 2012, *ApJS*, **199**, 12
 Melioli, C., de Gouveia Dal Pino, E. M., & Geraissate, F. G. 2013, *MNRAS*, **430**, 3235
 Molinari, S., Bally, J., Noriega-Crespo, A., et al. 2011, *ApJL*, **735**, L33
 Nakai, N., Hayashi, M., Handa, T., et al. 1987, *PASJ*, **39**, 685
 Shopbell, P. L., & Bland-Hawthorn, J. 1998, *ApJ*, **493**, 129
 Su, M., Slatyer, T. R., & Finkbeiner, D. P. 2010, *ApJ*, **724**, 1044
 Taylor, C. L., Walter, F., & Yun, M. S. 2001, *ApJL*, **562**, L43
 Veneziani, M., Elia, D., Noriega-Crespo, A., et al. 2013, *A&A*, **549**, A130
 Weaver, R., McCray, R., Castor, J., Shapiro, P., & Moore, R. 1977, *ApJ*, **218**, 377